Effect of Aging on the Mechanical Properties of Methacrylate 3D Printed Parts

Christian E. Rivera, C. R. Hasbrouck, Joseph Fisher, Joseph Bartolai, and Simon W. Miller

Applied Research Laboratory,

The Pennsylvania State University, University Park, PA 16802

Abstract:

The effects of natural and artificial aging processes on the mechanical properties of commercially available methacrylate photopolymer parts are explored in this paper. The specimens were produced with Grey Pro resin on a Formlabs Form 3L stereolithography (SLA) printer. A design of experiments was developed and the specimens were evaluated for: time elapsed since printing (green, 1 and 3 months), storage condition (ambient laboratory environment, darkened container), and aging process (ambient laboratory lighting, manufacturer suggested post-cure). The mechanical properties were characterized using uniaxial quasi-static tensile and microhardness testing to evaluate the experimental design. Additional microhardness maps were generated from cross-sections of bisected cubes to assess depth-of-cure and spatial gradients resulting from the aging process. After evaluation, preliminary results highlight the time, storage, and aging sensitivities of SLA-printed methacrylate photopolymer parts' mechanical properties in both bulk (tensile) and local (microhardness) measurements.

Keywords: Stereolithography (SLA) printing, SLA bulk and local properties, Aging of SLA parts, Methacrylate 3D printed parts

Introduction and Motivation:

Fabricating 3D printed parts with high precision and predictable mechanical properties is crucial for functional prototyping in additive manufacturing (AM). SLA printing, also known as resin 3D printing, provides high precision and excellent surface finish for parts made with liquid photopolymers. Consequently, resin 3D printing is utilized across various fields, including dental prototyping [1] and applied engineering sciences [2, 3]. In the engineering sciences sector, where resin 3D printing is employed, ensuring that prototypes meet expected mechanical properties is essential for experimental replicability. Understanding experimental variability and the changing parameters is critical for achieving reliable data. Manufacturers such as Formlabs offer material datasheets for their resins, detailing properties of green parts (as-built) and those post-cured (artificially aged through the manufacturer's recommended post-cure method) [4]. During SLA printing, parts are exposed to ultraviolet (UV) light, and can be post-cured (artificially aged) with heat and additional UV light to alter and improve their mechanical properties through photopolymerization [5]. Given the prevalence of UV light, it is important to determine how to properly store prints in their green state after removal from the printer's build plate. Similarly, understanding how deeply ambient laboratory light penetrates during the curing process and the effectiveness of the manufacturer's post-curing process is crucial.

To provide further context, consider an experiment investigating how various lattice geometries can enhance the structural capabilities or manipulate the expected mechanical response of a structure [6]. Ensuring stable material properties throughout the geometry of the resin-built part are essential for accurately assessing the effectiveness of the lattice structure. One approach might be to artificially age the part using a curing procedure. However, due to uncertainty about the depth of UV cure penetration and variability in lattice profiles (e.g., unit cell size and volume fractions), it is unclear whether every part will receive a uniform cure. Therefore, specimens with lattice infill used in prototyping should remain in their green state. Immediately after removal from the build plate and fabrication, the part should be expected to behave as a true green specimen.

To ensure that the expected mechanical properties are achieved, SLA 3D printed parts should be tested immediately after removal from the printer. However, this timing may be influenced by the availability of testing apparatus and technicians. SLA 3D printing can be time-consuming and potentially constrained by build plate size, which may necessitate multiple printing batches and result in significant downtime between prints. Consequently, testing parts in their true green state may be challenging or impractical. As a result, parts may rest for an unspecified duration before the testing apparatus or a full batch of specimens is ready. This introduces potential variability in how different storage conditions can affect deviations from the green properties.

Given these practical constraints, the study incorporates the analysis of intermediate aged states to bridge the gap between green and infinitely aged material properties. The purpose of including intermediate aged samples is to create a profile for material properties that fall between the green and infinitely aged states. By using the two baselines—green and infinitely aged—as boundaries for interpolating the properties of parts that have been allowed to age for a defined period, this study aims to capture how mechanical properties evolve over time. This approach provides a more comprehensive understanding of material behavior for parts that are not tested immediately but have aged under controlled conditions for a short period of time.

If there is a significant increase in mechanical properties over time due to prolonged exposure to ambient lighting conditions, this introduces additional variability into the experiment if not properly accounted for, making data replication more challenging. Similarly, the study of mechanical properties evolution through prolonged exposure should also consider the permeability of the resin and the depth of cure achieved by the part. Understanding how deeply UV rays penetrate during curing can provide valuable insights into the part's localized expected behavior. An uneven cure will result in a gradient of mechanical properties across the part's cross-section, adding another layer of variability to the experiment. Mechanical properties can be assessed through appropriate testing methods

This paper will detail the changes in both bulk and local properties through two types of testing on aged specimens. The first type involves assessing bulk properties through uniaxial tensile testing of ASTM D385 Type V specimens printed with Grey Pro resin (see Figure 1).

Specimens were mechanically tested at several stages: immediately after printing, 1-month after printing, 3 months after printing, and following artificial aging using the manufacturer's recommended curing procedure (designated as "infinitely aged"). Additionally, the effects of two storage methods on initially green parts were monitored over the specified time intervals. The second type of test to assess local properties involved cube specimens subjected to microhardness mapping using a micro-indenter to identify hardness gradients and depth of cure within sliced cross-sections, in accordance with ASTM E384. Understanding the impact of prolonged exposure on SLA-printed parts—including changes in mechanical properties and the resin's permeability with respect to depth of cure under UV light—provides valuable insights for replicating studies and addressing the temporal dependencies of these parts in mechanical testing. The Formlabs Form 3L was used for specimen fabrication, while the Form Cure L was utilized for artificial aging.

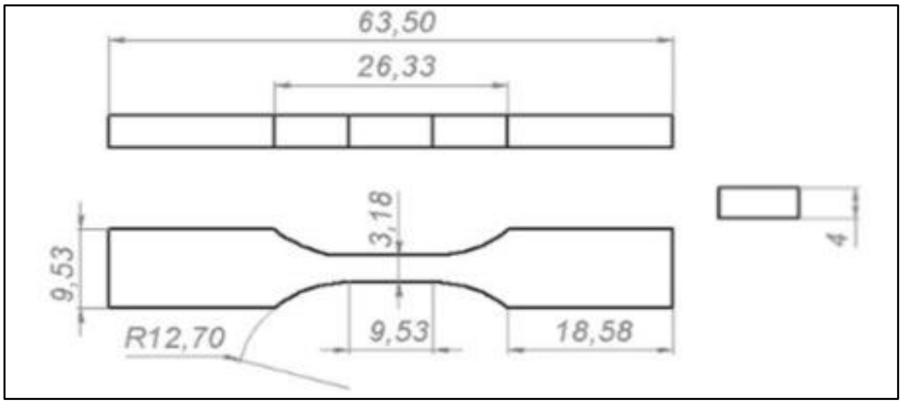

Figure 1: Dimensions for ASTM D385 Type V specimen

Procedure:

To investigate how the resin's bulk properties evolve over time, six test groups were prepared using specimens printed with the Form 3L. These specimens were printed at 50 micron layer height and with Grey Pro Formlabs resin. One group was exposed to ambient laboratory conditions, while another was kept in complete darkness. Each group was further subdivided based on aging duration, resulting in 1-month and 3-month subgroups for both the ambient and dark conditions. Additionally, two baseline groups were included: one as-built (green) and another that underwent a manufacturer-recommended curing process using the Form Cure L, representing the minimum and maximum expected bulk properties. The group subjected to UV curing with the Form Cure L was designated as "infinitely aged" and is contextually referred to as artificial aging. The specimens were subsequently subjected to uniaxial tensile testing to generate force versus displacement curves, facilitating comparison of bulk properties across the different groups. The aging parameters are summarized in **Table 1**.

Table 1: Summarized aging parameters for bulk properties

Aging Parameters						
Age	Green	1 month		3 months		Infinite
Storage Condition		*Dark*	*Light*	*Dark*	*Light*	
Aging Temperature	Room Temperature					

A total of 30 specimens were printed using the Form 3L, designed to comply with ASTM D638 Type V [7]. The printed specimens were tested under uniaxial tension using an Instron 3345. Strain was measured with a non-contact laser extensometer (model LE-05) manufactured by Electronic Instrument Research, which has a specified nonlinearity of ± 0.0004 inches. Each specimen was fitted with two thin strips of reflective tape across the gauge region, with each strip positioned at the end of one side of the gauge region.

The testing procedure began with the setup and calibration of the Instron 3345 and LE-05 to ensure accurate measurements. Data such as the specimen's width, gauge region thickness, and laser gauge length were entered into the Bluehill Central lab management software. The specimen was then carefully positioned in the Instron 3345, ensuring proper alignment of the LE-05 laser to bisect the gauge region accurately (see Figure 2 for specimen and LE setup). Initial offsets were zeroed out in the Bluehill software before applying a preload of approximately 1.5 pounds using the top grips to securely hold the specimen in place. Following this setup, the laser extensometer was zeroed to begin displacement measurements. The test was then initiated via the software, applying force at a uniform displacement rate of 0.1 in/min (to ensure quasi-static conditions) until the specimen fractured. Throughout the process, continuous data recording and consistent environmental conditions were maintained to ensure reliable results and facilitate future analysis for replicability.

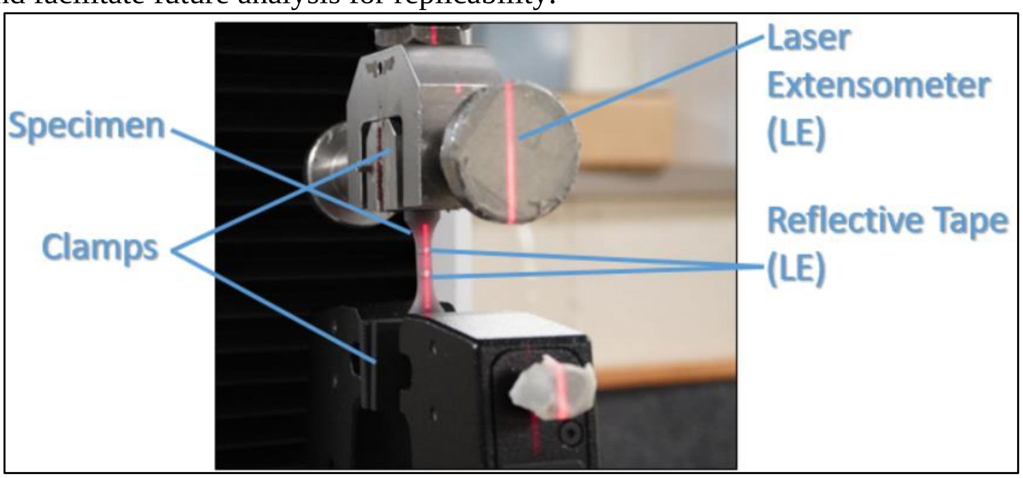

Figure 2: Specimen and LE setup

The investigation into the localized properties of Grey Pro resin involved printing four cubes of length ~0.707 inches (to have a hypotenuse of 1 inch). These cubes were evenly divided into two testing groups: one group remained in the green state, while the other was artificially aged using the Cure L machine following the manufacturer's recommended curing procedure for the resin. To prepare the specimens for micro-indentation analysis, each cube was bisected twice, resulting in four equally sized rectangular prisms per group. These prisms were then placed into 1-inch cold mounts, with the face that was originally internal to the cube being polished down to 1 micron. Microhardness mapping was conducted using a Q60 A+ Automatic Micro-indenter (see **Figure 3** for the micro-indenter apparatus). The Vickers indent testing method was used in accordance with ASTM E-384 [8] with the value being HV 0.05.

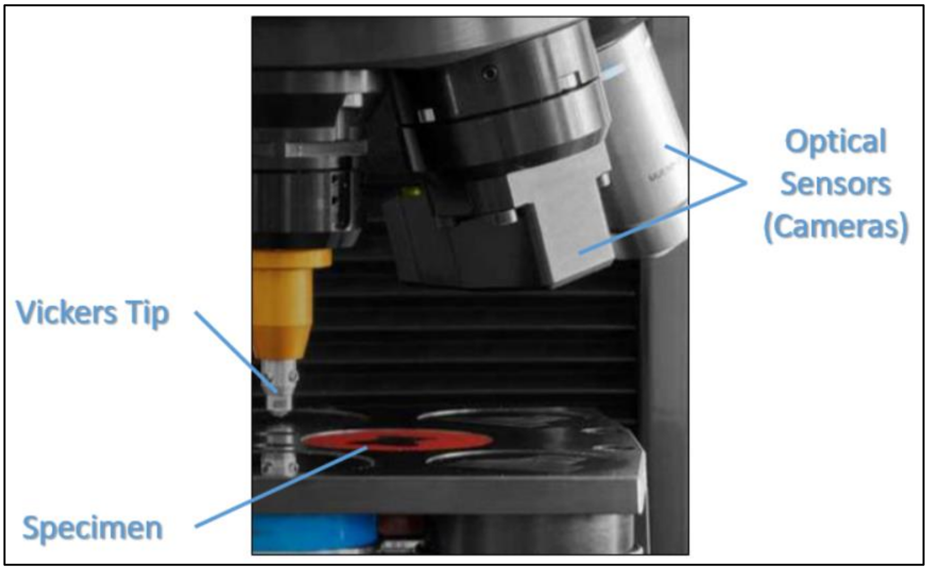

Figure 3: Q60 A+ Automatic Micro-Indenter

Results:

The tensile tests conducted on the Grey Pro resin yielded values for key bulk properties: Young's Modulus, Ultimate Tensile Strength (UTS), 0.2% Offset Yield Strength, and Strain at Break. The experimental conditions included different aging durations and storage environments. Specifically, the designations "1" and "3" denote aging periods of 1-month and 3 months, respectively. The designation "INF" refers to specimens subjected to artificial aging, colloquially termed as "infinitely aged." Storage conditions were classified as "MD" for months stored in darkness and "ML" for months stored under light exposure. It is important to note that for the INF, 3MD, and 1ML groups, one specimen from each category was excluded from the analysis due to slippage from the clamps during tensile testing. This exclusion was necessary to ensure the accuracy and reliability of the reported data.

Table 2: Young's modulus for each aged and subset storage conditions

Modulus	Average (psi)	Standard Deviation	95% CI	Report
Green	209497.98	8239.74	2.57	209498 ± 21181 psi
1MD	269006.98	11290.86	2.78	269007 ± 31348 psi
1ML	283660.56	16496.15	2.57	283661 ± 42405 psi
3MD	285504.44	8096.22	2.57	285504 ± 20812 psi
3ML	305835.73	12386.45	2.78	305836 ± 34390 psi
INF	376690.26	16243.35	2.78	376690 ± 45099 psi

Table 2 presents the Young's Modulus values, which indicate a notable increase with extended UV exposure. Specifically, specimens aged for 1-month demonstrated a 5.2% increase in Young's Modulus when stored under light compared to those stored in darkness. For specimens aged for 3 months, the modulus increased by 6.6% under light conditions. Over a 2-month period, specimens stored in darkness showed a 5.7% increase from the 1-month dark group, whereas those exposed to light exhibits a 7.2% increase from the 1-month light group.

Table 3: Ultimate tensile strength for each aged and subset storage conditions

UTS	Average (psi)	Standard Deviation	95% CI	Report
Green	5204.13	131.42	2.57	5204 ± 338 psi
1MD	5455.98	156.06	2.78	5456 ± 433 psi
1ML	5923.94	186.05	2.57	5924 ± 478 psi
3MD	6034.95	128.50	2.57	6035 ± 330 psi
3ML	6212.24	197.47	2.78	6212 ± 548 psi
INF	8926.38	294.66	2.78	8926 ± 818 psi

Table 4: 0.2% Offset yield strength for each aged and subset storage conditions

0.2% Offset Yield	Average (psi)	Standard Deviation	95% CI	Report
Green	4884.51	270.57	2.57	4885 ± 696 psi
1MD	4968.68	196.62	2.78	4969 ± 546 psi
1ML	5116.13	225.39	2.57	5116 ± 579 psi
3MD	5055.75	131.40	2.57	5056 ± 338 psi
3ML	5182.01	290.95	2.78	5182 ± 808 psi
INF	8580.53	331.99	2.78	8581 ± 922 psi

Tables 3 and **4** reveal that both Ultimate Tensile Strength and 0.2% Offset Yield Strength increase with prolonged UV exposure. Furthermore, storage conditions have a significant effect on these properties. For specimens aged for 1 month, those stored under light showed incremental improvements in tensile and yield strengths compared to those stored in darkness. This trend is more pronounced in the specimens aged for 3 months, with higher values observed under light conditions.

Table 5: Strain at break for each aged and subset storage conditions

Strain at Break	Average (in/in)	Standard Deviation	95% CI	Report
Green	27.11	2.96	2.57	27.1 ± 7.62 %
1MD	25.86	1.34	2.78	25.9 ± 3.71 %
1ML	22.98	1.08	2.57	23 ± 2.77 %
3MD	23.69	1.18	2.57	23.7 ± 3.04 %
3ML	23.02	1.72	2.78	23 ± 4.76 %
INF	14.38	1.04	2.78	14.4 ± 2.88 %

Table 5 indicates a decrease in Strain at Break with increased UV exposure, reflecting an increase in brittleness. This is consistent with the polymerization effects induced by prolonged UV exposure, which contribute to the material's increased rigidity and decreased flexibility.

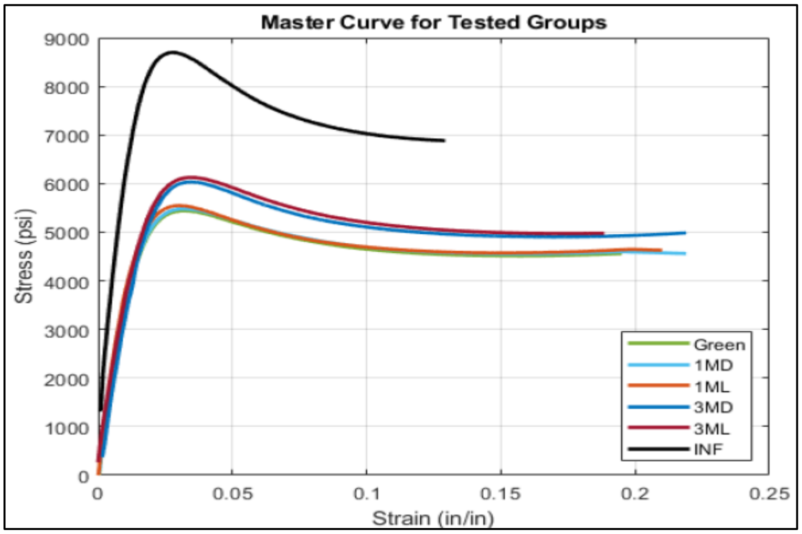

Figure 4: Master curve plot for all of the aged specimen groups

Figure 4 illustrates the master curve for the aged specimen groups, showing deviations between groups aged under different conditions. The truncation observed in the master curves reflects the lower Strain at Break values reported in **Table 5**. This is the consequence of the interpolation performed between 4-5 specimens in each group to generate the respective master curves for each tested group.

Within the hardness study, we investigated the local hardness properties of cubes printed with Grey Pro resin to assess the depth of cure within a solid part subjected to the manufacturer's recommended curing process. The hardness values of artificially aged specimens were compared against a baseline set of green specimens, which were expected to exhibit uniform hardness throughout their thickness. This comparison provides insight into the expected deviations in hardness for the cured specimens that are assumed to be fully cured throughout its complete thickness.

To perform this analysis, an array of 11 measurement points was used along a straight line across the middle of the bisected cross-section of the artificially aged specimens. For the green specimens, only 5 measurement points were utilized. The measurement direction focused on the shortest side of the rectangular prism, with points starting from the outermost surface (blue) and extending inward towards the center (red). Figure 5 illustrates the trajectory of the indenter during the test.

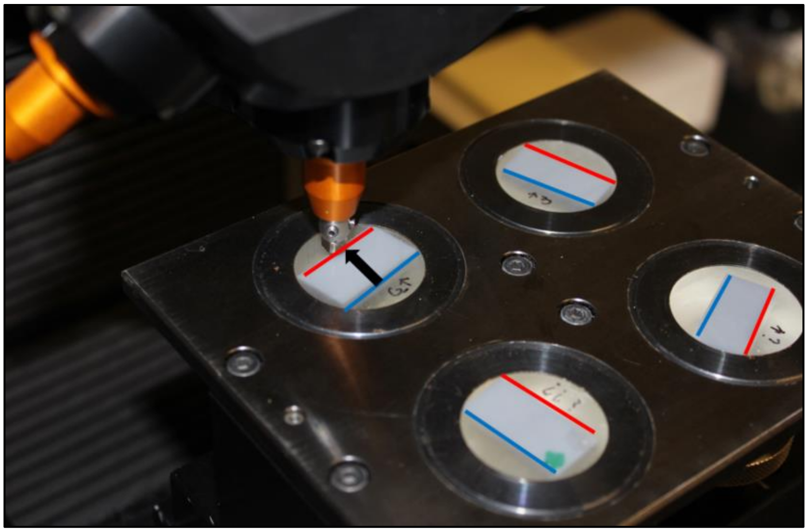

Figure 5: Direction of indenter visualization

The indentation testing involved 2D area mapping using a load of 0.110 lbf (HV 0.05). Data acquisition and image processing were fully automated with Qpix CONTROL2. Consistent with protocols established for bulk property tests, continuous data recording and controlled environmental conditions were maintained to ensure result reliability and support future replication.

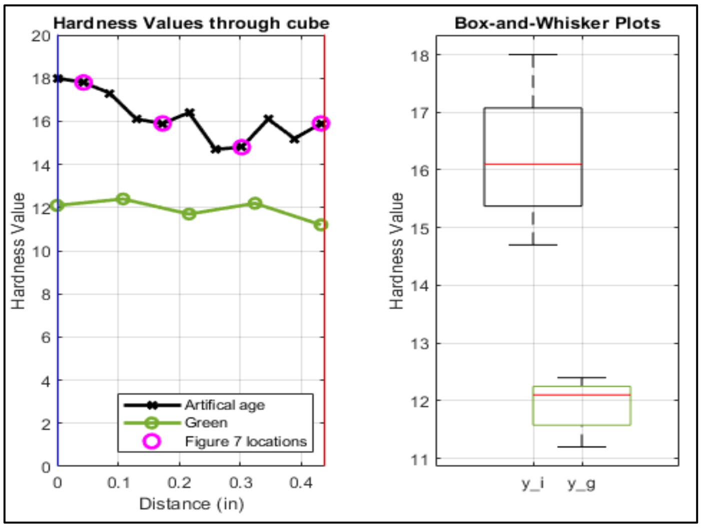

Figure 6: Hardness values through the cube and the value distribution

The recorded hardness values, ranging from the blue to red locations across the specimen, are graphed in Figure 6. This figure also shows the distribution of values to illustrate deviations among tested points. The box plot for the green specimens indicates the expected magnitude of deviation for a uniform hardness distribution. Notably, the artificially aged specimens exhibited a larger deviation from uniform hardness than anticipated, suggesting significant variability in hardness across the indenter's travel region. Despite having fewer points, the green specimens still demonstrate that the artificially aged specimens show a clear decrease in local hardness as the measurement progresses deeper into the part.

Table 6 summarizes the average hardness values, standard deviations, and 95% confidence intervals for both the artificially aged and green specimens. The data reveal a substantial difference in standard deviation, highlighting increased variability in hardness values across the depth of the cured specimens.

Table 6: Hardness value through the cross section for the artificial aged and Green specimens

Hardness Value	Average	Standard Deviation	95% CI	Report
Artificial Age	16.20	1.12	2.20	16 ± 2
Green	11.92	0.48	2.57	12 ± 1

The Vickers hardness values determined for the cured (artificially aged) and green specimens were 16.2 HV 0.05 and 11.9 HV 0.05, respectively. Unfortunately, the manufacturer's material data sheets do not provide hardness values for direct comparison, as they do for bulk properties. Therefore, there is currently no direct reference point for validating these hardness measurements against manufacturer specifications.

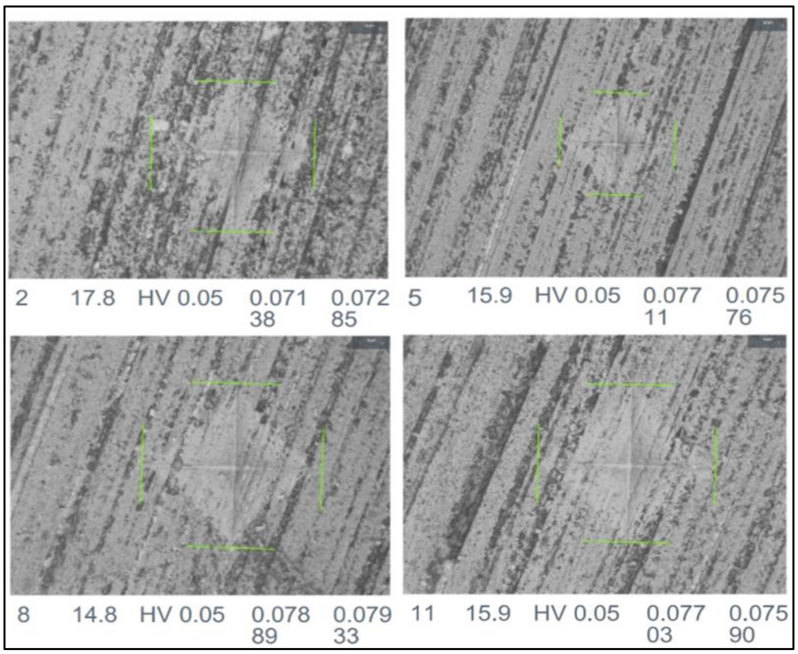

Figure 7: Microhardness surface for the artificial aged specimen (cured)

Figure 7 presents selected points along the indenter's path from Figure 6 to highlight discrepancies in hardness measurements. Notably, hardness values at point 5 and point 11, despite point 11 being positioned deeper into the part and thus expected to be softer, were found to be identical. This anomaly may be attributed to inconsistencies in surface finish, which could have led to non-uniform indentation locations and potentially interfered with the accuracy of the Vickers hardness testing. In contrast, the green specimen, which exhibited a similarly poor surface finish as shown in Figure 8, demonstrated a lower deviation in hardness measurements. This may be due to the more uniform or patterned distribution of surface irregularities, which could have reduced the impact of surface imperfections on the Vickers indenter, thereby yielding more consistent hardness values.

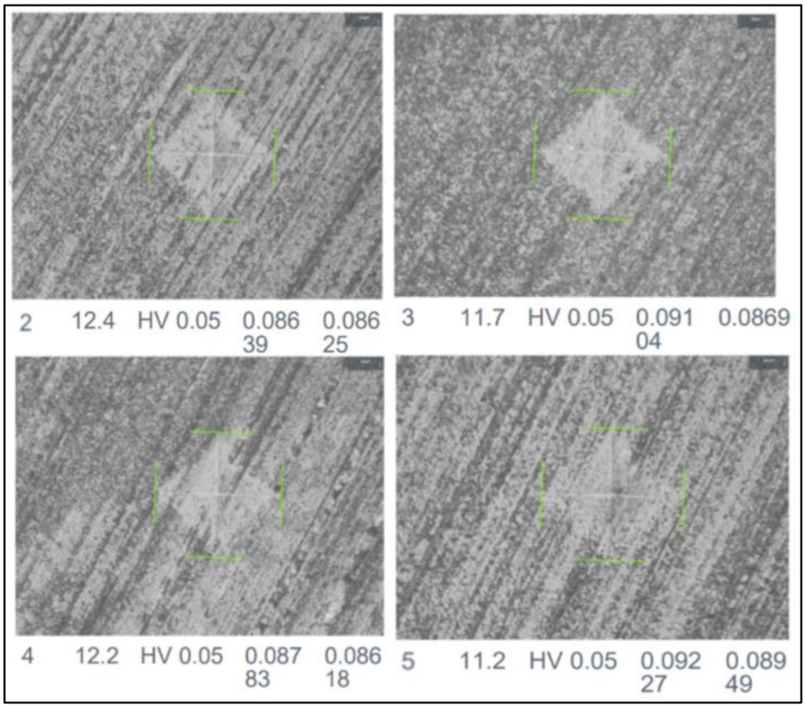

Figure 8: Microhardness for the green specimen

Figure 8 shows the microhardness distribution for the green specimen, illustrating the differences in measurement consistency between cured and uncured states. Although uniform hardness was anticipated for the cured specimen, the manufacturer's UV curing process—designed to penetrate the full thickness of the resin—may not have achieved complete effectiveness. The observations suggest potential sources of variability in the standard deviation of hardness measurements for the artificially aged specimens. Despite the surface finish challenges, the green specimens consistently demonstrated a Vickers hardness value of approximately 12 HV 0.05, indicating relative uniformity in hardness. This implies that the cured specimens likely exhibited significant spatial gradients in local hardness, suggesting incomplete uniformity in curing through the thickness of the part.

Conclusion:

This study explores the impact of natural and artificial aging on the mechanical properties of SLA-printed methacrylate photopolymer parts, using Grey Pro resin on a Formlabs Form 3L printer. Through a well-structured experimental design, the research assessed the effects of various aging durations, storage conditions, and curing processes on the mechanical properties of these parts. The evaluation encompassed both bulk properties via uniaxial tensile testing and local properties through microhardness mapping.

The results demonstrate a significant impact of aging and storage conditions on mechanical properties. Notably, there is an observable increase in Young’s Modulus, Ultimate Tensile Strength (UTS), and 0.2% Offset Yield Strength with extended UV exposure, while Strain at Break decreases, reflecting increased rigidity and decreased flexibility. Storage conditions also play a critical role, with light exposure generally resulting in better mechanical performance compared to darkness. The microhardness tests further revealed notable differences in hardness gradients, indicating variability in the depth of cure and uniformity of the curing process.

Despite these insights, this study did not interpolate mechanical properties for specific durations between green and infinitely aged states. The inclusion of intermediate aged samples—both under dark and light conditions—was intended to provide a framework for approximating the expected evolution of mechanical properties over time. These intermediate states serve as valuable references for understanding material behavior at various aging stages, offering a practical method for approximating properties of parts that are not immediately tested.

To enhance the robustness of future investigations into the aging effects on SLA-printed parts, several refinements can be made. Firstly, incorporating detailed interpolation techniques for various aging intervals would provide a more precise estimation of mechanical properties between green and fully cured states, thus improving the accuracy of property predictions. Expanding the range of aging conditions and durations, including different levels of UV exposure and environmental factors, would offer a more comprehensive understanding of the material's behavior under diverse scenarios. Additionally, increasing the number of measurement points in microhardness testing and comparing these with manufacturer data, if available, would enhance the reliability of local property assessments. Lastly, investigating methods for achieving a more uniform cure—such as refining curing techniques or exploring alternative material formulations—could mitigate variability in hardness and other mechanical properties, leading to more consistent results. These improvements would contribute to a more thorough understanding of SLA-printed material behavior and support the development of more reliable and accurate prototyping processes.

Citations:

[1] van Noort, Richard. "The Future of Dental Devices Is Digital." *Dental Materials*, Elsevier, 26 Nov. 2011, www.sciencedirect.com/science/article/abs/pii/S0109564111008955.

[2] Martinez, Pamela Robles, et al. "The History, Developments and Opportunities Of ..." *Researchgate*, Aug. 2018, www.researchgate.net/publication/326863794_The_History_Developments_and_Opportunities_of_Stereolithography.

[3] Mondschein, Ryan J., et al. "Polymer Structure-Property Requirements for Stereolithographic 3D Printing of Soft Tissue Engineering Scaffolds." *Biomaterials*, Elsevier, 6 June 2017, www.sciencedirect.com/science/article/abs/pii/S014296121730399X.

[4] "Material Data Sheet: Grey Pro." *Formlabs-Media.Formlabs.Com/Datasheets/Grey_Pro_Technical*, FORMLABS, 22 Jan. 2018, formlabs-media.formlabs.com/datasheets/Grey_Pro_Technical.pdf.

[5] Rashid, Ans Al, et al. "VAT Photopolymerization of Polymers and Polymer Composites: Processes and Applications." *Additive Manufacturing*, Elsevier, 11 Sept. 2021, www.sciencedirect.com/science/article/pii/S2214860421004395.

[6] Fisher, Joseph W., et al. "Catalog of Triply Periodic Minimal Surfaces, Equation-Based Lattice Structures, and Their Homogenized Property Data." *Penn State*, Elsevier BV, 22 Sept. 2023, pure.psu.edu/en/publications/catalog-of-triply-periodic-minimal-surfaces-equation-based-lattic.

[8] "Standard Test Method for Tensile Properties of Plastics." *Compass*, World Trade Organization Technical Barriers to Trade (TBT) Committee, 21 July 2022, www.astm.org/d0638-22.html.

[8] "Standard Test Method for Microindentation Hardness of Materials." *Compass*, World Trade Organization Technical Barriers to Trade (TBT) Committee, 8 Nov. 2022, www.astm.org/e0384-22.html.